

Mapping Phase Space Within a Glass Box Using Gold-Coated Melamine Formaldehyde Particles (August 2013)

*Kristin J. Sperzel, Jorge Carmona-Reyes, Michael Cook, Jimmy Shmoke, Lorin S. Matthews, and
Truell W. Hyde*

*Center for Astrophysics, Space Physics and Engineering Research, Baylor University, Waco, Texas
76798-7310, USA*

Abstract—Many dusty plasma experiments have been performed using non-conducting dust particles. In experiments reported in this paper gold dust is used to discover whether conduction plays an important role in dusty plasma or not. The gold particles are dropped into a ½ inch glass box. With an emphasis on phase space, the main goal of this research is to find out what the conditions are inside the glass box. Gold dust particles are dropped inside a GEC RF reference cell into the glass box and behaviors of the particles are monitored as system parameters are adjusted. The data is then analyzed using different types of software to obtain numerical information about the observed behavior.

Index Terms—Complex plasma, dust charge, particle coagulate, and sheath edge.

I. INTRODUCTION

It is estimated that 99.9% of observable matter in the Universe is plasma [1]. However, earth's atmosphere is not an environment where plasma often occurs naturally since kinetic to potential ratio conditions are not ideal for plasma production. Thus, a controlled plasma environment is produced in the lab to study and understand its dynamics and interaction with all other matter. Plasma is a state of matter in which the kinetic energy surpasses the ionization energy of molecules, which occurs by heating ordinary gas [2]. Plasma consists of ionized molecules and electrons; the plasma, in

theory, should have an equal number of electrons and ions. For every electron charge that gets separated from the molecule there should be an equal and opposing positive charge from the ion. Thus, the plasma is referred to as quasineutral or electrically neutral. The electrons move about with greater speed and mobility than the ions due to the electrons' mass being smaller than the mass of the ions. Dusty plasma physics, also known as complex plasma physics, involves microparticles (dust) being immersed into plasma. It is useful to study dusty plasma to figure out how material in space interacts with plasma. The microparticles obtain an overall negative charge because electrons are colliding with the dust more frequently than the ions due to the electrons greater speed and mobility. Many dusty plasma experiments have been performed in a lab-controlled environment. A controlled environment used to do experiments in is a Gaseous Electronic Conference (GEC) radio frequency (RF) reference cell and melamine formaldehyde micron size particles are often used in dusty plasma experiments; this will be explained in section II. The melamine formaldehyde particles are spherical and non-conducting, however, using gold-coated melamine formaldehyde particles allows for comparison with the many experiments performed using melamine formaldehyde particles [3], [4]. The comparisons will lead to a deeper understanding of plasma physics because conducting and non-conducting particles are being compared to understand the effect of charge arrangement on the micron size particles and its impact on dusty plasma interaction.

In this article experiments performed using gold-coated melamine formaldehyde particles inside a ½ inch glass box will be covered. The box has four walls with a wall thickness of 2mm. In section III the experimental method used for the experiments will be discussed. In section IV the results of the experiment will be brought forth. In section V there will be an analysis of the results. Finally, in section VI the significance of the analyzed results will be covered through discussion and conclusion.

Manuscript received August 2013. This work was supported by the National Science Foundation under Grant No. ***** through the Research Experience for Undergraduates program. This work was also supported by the Center for Astrophysics, Space Physics, and Engineering Research at Baylor University.

Kristin J. Sperzel is with St. Cloud State University, St. Cloud, MN 56301 USA and was a participant in the REU program (e-mail: spkr1001@stcloudstate.edu).

Jorge Carmona-Reyes is with the Center for Astrophysics, Space Physics, and Engineering Research, Baylor University, Waco, TX 76798 USA (e-mail: Jorge_Carmona_Reyes@baylor.edu).

Truell W. Hyde is with the Center for Astrophysics, Space Physics, and Engineering Research, Baylor University, Waco, TX 76798 USA (e-mail: Truell_Hyde@baylor.edu)

Lorin S. Matthews is with the Physics department at Baylor University, Waco, TX 76798 USA (e-mail: Lorin_Matthews@baylor.edu)

II. BACKGROUND

In 1994, three research groups reported observations of two-dimensional lattice crystals in dusty plasma [5]. An image of a two-dimensional lattice crystal can be found in Figure 1. These crystals are created due to two horizontal confinement forces, gravity, and the electrostatic force acting on the particle. While gravitational force pushes the particles down, the electrostatic force from an electrode pushes the particles up and the particles arrange themselves equidistantly due to the negative charge of each particle. Most of the phenomena observed in dusty plasma experiments can be explained by the balancing of forces acting on the melamine formaldehyde particles, the main forces being the gravitational force and the electrostatic force [6].

$$mg = QE \quad (1)$$

This balance occurs in a layer of the system called the sheath [7]. There are two important, yet to be completely understood, components of dusty plasma that are discussed in this paper; the sheath region and charging of dust particles inside the sheath. The sheath region is non-neutral, unlike the quasineutral plasma. In the sheath region the ion density is large compared to the electron density [8]. It is ion rich due to positive ions streaming from the plasma towards the negatively biased lower electrode. It is thought the potential of the sheath in the reference cell is modeled as parabolic; meaning the electric field in the sheath region is linear [9]. However, according to available literature [6], a more complex sheath model is required to have a better understanding of the physics in that region. It stated that the potential of the sheath might be better fit with a third order polynomial [6]. In order to simply finding the charge of a particle, a second order polynomial was used to model the sheath edge. For the experiments covered in this paper a 0.5-inch glass box was used. This box also introduces a new level of complexity due to the vertical restrictions that the glass box creates. The walls of the box create vertical restrictions because the fast moving electrons collide with the walls of the box and create negatively charged surfaces. This consequently

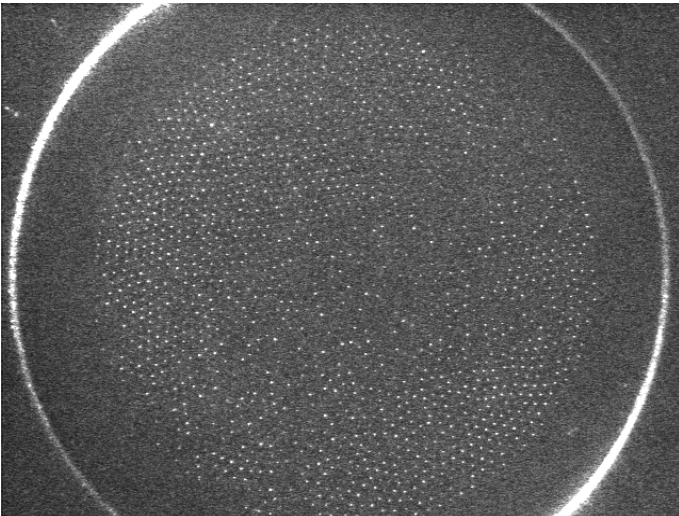


Fig. 1. Top view of a lattice crystal made of 8.89-micron melamine formaldehyde dust.

leads to the formation of a potential well with horizontal and vertical confinement bounds. The vertical confinement makes it possible to create particle chains within the box.

III. EXPERIMENTAL METHOD

A. Equipment

The experiments reported here were performed on the CASPER modified GEC RF reference cell that has been used previously for non-coated melamine formaldehyde dusty plasma, two examples can be found in [10], [11]. The reference cell chamber is made of stainless steel and has eight ports made with removable glass covers. Inside the cell there is a top grounded electrode used for stability and a bottom RF driven electrode, which are used to generate argon plasma at a frequency of 13.56MHz [12]. An image of a GEC RF reference cell can be found in Figure 2 and diagram of inside the reference cell can be found in Figure 3. Before conducting an experiment the cell is brought to high vacuum (10^{-7} Torr region) to eliminate foreign substances from the system. The cell pressure reduces to high vacuum by using a cryogenic pump. A cryogenic pump uses a cold surface of about 12K to condense gas and reduce the pressure of the cell. Once the cell is clean the pressure inside the cell can be raised after closing the high vacuum valve. Closing the high vacuum valve protects the cryogenic pump from pressures greater than 10^{-4} T. The chamber is then filled with argon and pressure within the cell is regulated with a roughing pump and butterfly valve. A mass flow controller regulates the flow rate of argon in the system. The flow rate is measured in standard cubic centimeters per minute (SCCM). The flow rate is generally set around 20 SCCM for the experiments that will be discussed in this section. A RF amplifier is used to drive the lower electrode and the RF network impedance is set at 50 Ohms (Ω) to maximize power transport efficiency. The power and other system parameters can be monitored using 4 oscilloscopes. One oscilloscope monitors voltage, current and derivative probes going into the cell, a second oscilloscope monitors the voltage being sent to the system and reflective voltage at the matching network, a third oscilloscope monitors

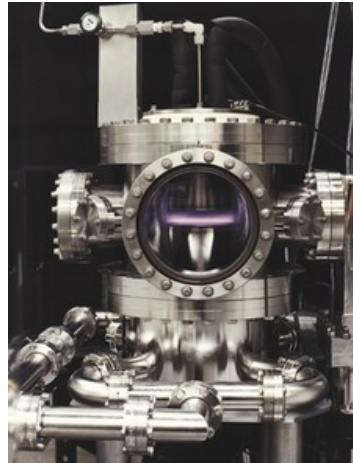


Fig. 2. An image of the exterior of a GEC RF Reference cell. Image Source [16].

DC bias, and a fourth oscilloscope monitors system power before it goes into the amplifier and after the power is manipulated by the amplifier. As stated in the background, for the experiments discussed in this paper a glass box is placed on the center of the cell's bottom electrode. A diagram of the cell and the glass box can be seen in Figure 3.

Once plasma is ignited, the plasma is left glowing at

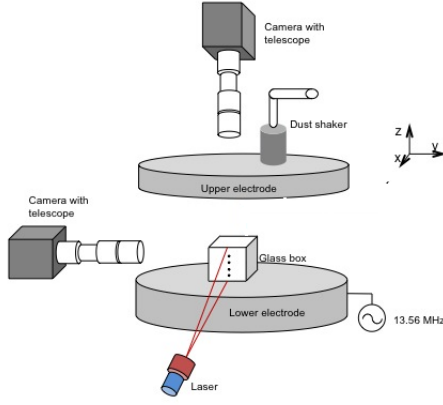


Fig. 3. The set up of the GEC RF Reference Cell including the glass box, the dimension of the glass box is 0.5-inches. Image source, [3].

maximum power in order for the system to stabilize. Next, gold-coated, $8.93\mu\text{m}$, melamine formaldehyde dust particles are dropped into the reference cell by manually tapping the top of a movable lever with a dust dropper attached to the end. After dust is in the cell the dust dropper is moved out of the way to prevent excess dust from falling in. The camera used to record the experiments is the FASTCAM 1024 PCI. This is a high-speed camera that uses a CMOS sensor. The lens used was an Infinity K2/DistaMax lens. A 2X TR tube was also used to get double the magnification for most of the experiments. The camera was placed on the outside of one of the eight ports.

Two software programs are used to assess the data obtained in these experiments. The first program is ImageJ; a program that is used to process images. An ImageJ plug-in called Particle Tracker tracks particles in an image set and produces the x and y coordinates of the particle for each frame in a set. These coordinates are put into the second program in MATLAB. This program takes the positions of the particles, finds the difference in position between two frames and multiplies this by the camera frame rate. Then the program multiplies the difference between two consecutive velocities by the frame rate for the image set.

B. Electronic Data and Plasma Power

LabVIEW is used to record data from the four previously mentioned oscilloscopes, this is later used to calculate plasma power, which is essential for experiment repeatability since setting the system at the same system power for every experiment may not result in the plasma power. GEC reference cell plasma parameters are monitored with voltage and current probes as well derivative probes and recorded by using an in-house developed LabVIEW program. Using Eq. (2) plasma power is obtained and Eq. (3) is used to compare system output voltage to the plasma power.

$$-30\text{dB} = 10\log\left(\frac{P_{out}}{P_{in}}\right) \quad (2)$$

$$P = \frac{V^2}{R} \quad (3)$$

In Eq. (2) P_{out} is the power is the output power or system power and P_{in} is the input of power recorded by the probe or plasma power.

Comparing the plasma power and system power it was found that the plasma power for our system is about 42% of the system power. This is a significant difference in power. It is important to know what the plasma power is so that experiments can be repeated as accurately as possible in other reference cells.

C. Experiment One – Single Particles or Coagulates In a Glass Box

This experiment involved several variations of having one $8.93\mu\text{m}$ gold coated particle in the glass box. The pressure was set to 108mT, this will be the pressure for the majority of the experiments covered in this paper. 108mT is the experimentally found pressure that creates the most stable particle chains in the specific GEC RF reference cell that was used for the experiments in this paper. The system was set to the maximum power of 29.8W where the plasma power was 12.3W. Over a course of about 4.5 seconds the system power was lowered from maximum power to 1.39W where the plasma power was 0.63W. 4.5 seconds is the time it took for gravity to overcome QE, resulting in the particle dropping to the lower electrode. Next, a different singular particle was put in the box and the same procedure was followed. The system was set to a maximum power of 29.8W where the plasma power was 12.3W. Over a course of about 8 seconds the system power was lowered to 1.06W where the plasma power was 0.48W. About 8 seconds is the time it took for gravity to become greater than the QE force. The behavior was recorded with the high-speed camera at 500fps.

D. Experiment Two – Particle Chains

For this experiment $8.93\mu\text{m}$ gold-coated particles were dropped into the glass box, after stabilizing, the particles formed a chain; the chain consisted of seven particles. The pressure within the system was 108mT. The system power was set at 1.25W with a plasma power of 0.56W. The three topmost particles were stable and the other four particles were

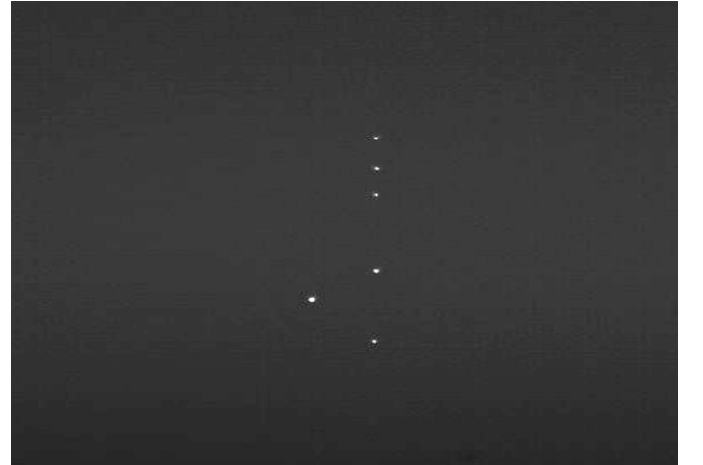


Fig. 4. An image of the particle chain with the orbiting particle to the left of the chain, it is shown that the top three particles are stable and have very equal spacing.

not. An image of the chain can be found in Figure 4. The fourth particle of the chain orbited horizontally where the chain seemed to be the axis of rotation. Five different sets of images were taken at an average of 12 minutes apart. The side view of the behavior was recorded with a high-speed camera at 500fps.

E. Experiment Three – Sheath Edge

The particles that were used for experiment three were melamine formaldehyde particles with a diameter of $.46\mu\text{m}$. The small particles were used to find the sheath height. It is thought that smaller particles levitate near the sheath edge, and the larger particles converge to this height as the RF voltage increases [6]. The particles were dropped into the cell; the high-speed camera took images of the particles levitating at a speed of 60fps. The pressure was set to 108mTorr for each variation of this experiment. The system power was varied starting at 1.25W to the maximum power of 29.8W in seven increments. The height of the center of mass of the particles was then used to estimate the height of the sheath for each of the seven variations.

F. Experiment Four – Free Fall

The particles that were used for experiment four were $8.9\mu\text{m}$ gold-coated particles. The particles were dropped into the reference cell at varying powers in order to measure the electric force acting on the particles. Initially the particles were dropped in with no system power. This was done to ensure that the acceleration recorded with out power matched the gravitational value of 9.81m/s^2 within error. The plasma was then ignited and left to stabilize. The system power was varied from 1.25W to 2.66W throughout the first variations. Next, the DC bias was varied separately from -10.25V to -30.75V through out the second variations. The experiments for each variation were recorded with the high-speed camera at 1800fps. Outside the port opposing the camera lens a floodlight was shined through the reference cell towards the camera. This allowed us to see the silhouettes of the dust particles to more accurately track them.

IV. RESULTS

A. Experiment One Results

The two particles in this experiment exhibited significantly different behavior. The differences in the behaviors were the amount of time it took for the gravitational force to take over the electrostatic force acting on the particles, the velocity in the x direction of the particles, and the brightness of the particles. For the first particle the gravitational force became greater than the electrostatic force in a much smaller amount of time. It can be seen that the gravitational force is greater than the electrostatic force when the particle is no longer able to levitate. The force of gravity being greater than the opposing electrostatic force causes the particle to fall to the lower electrode. When this happens both velocity and acceleration in the y direction of the particle increase greatly in magnitude. The difference in time could have been from human error in lowering the power by hand. However, the time it takes the first particle to drop to the lower electrode

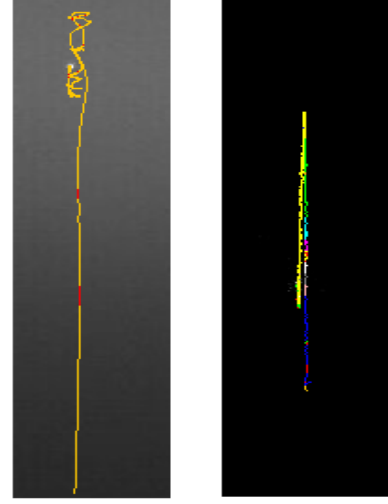


Fig. 5. Trajectories of particle one (coagulate) and particle two, the movement in the x direction in particle one is shown to be greater than particle two

(4.5 seconds) is about half the time it takes the second particle to drop to the lower electrode (8 seconds) so it is less likely that this is due to human error.

The trajectories done by Particle Tracker in ImageJ of the first and second particle can be found in Figure 5. In Figure 5 it is shown that there is significant oscillatory movement in the x direction for the first particle. It is also shown that there is little movement in the x direction for the second particle. This visual movement was supported numerically, and the plots of the numerical results are shown in Figures 6 and 7. In Figures 6 and 7 the x position of particle 1 and particle 2 are plotted against time.

The illumination of the particle was also plotted on Figures 6 and 7 in order to show correlation in plasma power and particle position. The first particle, with the relatively large amount of movement in the x direction, appeared to be much brighter than the second particle. The first particle was zoomed in on to analyze and appeared to be a coagulate of particles rather than a single particle. The particle was asymmetric and took up many more pixels than the second particle, which was spherical. The first particle took up nine pixels while the second particle took up one pixel. The error root-mean-square error for the accuracy of particle location within pixels is somewhere between .02 and .14 pixels per particle [13]. Both particles had unexpected movement in the y direction. The movement was unexpected because it is well accepted and observed that, when the glass box is not present, as the power lowers, the negative potential on the lower electrode lowers, and the particle becomes less repelled by the bottom electrode. The particle continuously decreases in height until the electrical force is smaller than gravity, causing the particle to fall to the lower electrode. As the power was lowered in this experiment, the particles traveled down initially and then up, and finally down again as the particles fell to the electrode rather than continuously falling down. This indicates that this is occurring due to conditions of the phase space that only occur within the glass box.

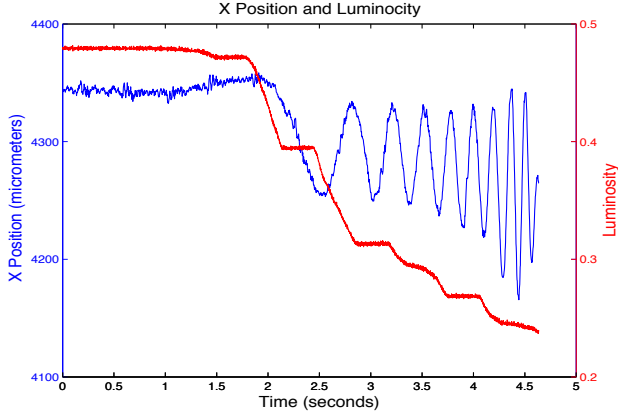


Fig. 6. Position of the first particle coagulate's horizontal position as power is being lowered. Luminosity is shown as a gauge to the value of plasma power as it was being lowered.

B. Experiment Two Results

There were five different image sets recorded of the particle chain. For the first three sets of images the particle was made up of six non-orbiting particles and one orbiting coagulate, after the third image set the bottom particle fell to the bottom electrode and the particle chain consisted of five non-orbiting particles and one orbiting coagulate for the next two image sets. The orbiting coagulate was of most interest in this experiment. Using Particle Tracker in ImageJ the x and y position of the orbiting coagulate was recorded; orbits of the coagulate were then found by taking the lowest and greatest x positions. The frequencies of the orbits were calculated using the amount of frames it took for an orbit multiplied by 1/1800 seconds per frame. It was found that the frequency of the orbit varied inversely with the radius of the orbits, which indicates that angular momentum is conserved. Table 1 shows data for the radius-frequency relationship. The radius and frequency of the orbits were used to calculate angular momentum, torque, and the electric force acting on the particle at the height of the orbiting particle coagulate. Table 1 shows an example of calculations from the data in experiment two. This was done using the following Eq. (4)-(6).

Table 1

Radius	Frequency	Angular Momentum	Torque	F_e
1.1E-3	3.90	1.88E-17	-1.6E-17	-1.4E-14
9.7E-4	3.84	1.40E-17	-2.7E-17	-2.7E-14
7.8E-4	3.68	7.09E-18	5.11E-17	7.2E-14

The standard deviation of angular momentum was .006 for this set of images. Radius is measured in meters (m), frequency is measured in Hz, angular momentum is measured in Nms, torque is measured in Nm, the electric force is measured in Newtons (N).

$$\ell = \mathbf{r} \times \mathbf{mv} \quad (4)$$

$$\tau = \frac{d\ell}{dt} \quad (5)$$

$$F_e = \frac{\tau}{r} \quad (6)$$

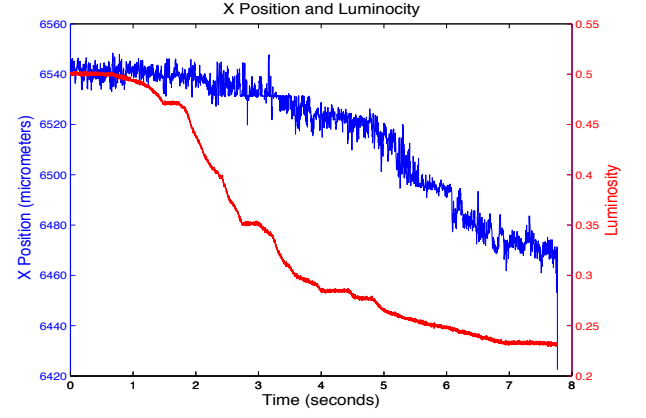


Fig. 7. Position of the second particle horizontal position as power is being lowered. Luminosity is shown as a gauge to the value of plasma power as it was being lowered.

During a related experiment it was observed that when RF power was increased the particle chain turned into a cluster and immediately after power was decreased to the previous setting; this process redistributed the location of the orbiting particle within the new-formed chain. Effectively using this process, the orbiting particle could be moved to any of the bottom four positions in the particle chain and used for mapping the electric field at any of those positions.

C. Experiment Three Results

The sheath height was recorded for seven different powers. The sheath height initially increased with power and then decreased with power after a plasma power of 2.29W. The measurements of the sheath height were consistently above the height of the orbiting coagulate. The value of the sheath height at the system power that was used in experiment two (1.25W) was 7.6E-3m. Using the measured sheath height the charge of the particle was calculated using an Eq. (7). In Eq. (7), h_b is the position of the sheath edge, h_{eq} is the equilibrium height, V_p is the potential at the electrode, and V_b is the potential at the sheath edge. The density, ρ , is 1643.3Kg/m³ and the radius of

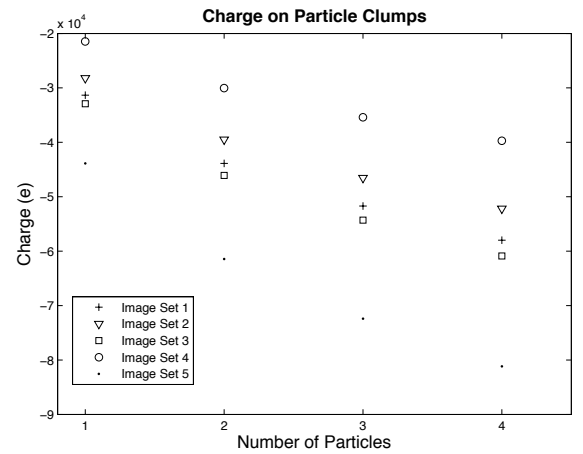


Fig. 8. Calculated charge on particle coagulates for each image set, the x-axis shows the number of particles in the coagulate and the y-axis shows the amount of charge on the coagulate

one particle is $4.465\mu\text{m}$. Since we have a particle coagulate rather than a particle, and are estimating the particle coagulate to be two to four particles, the charge for the particle coagulate is calculated using a linear equation. This equation and origin of the equation is demonstrated [14]. The charge calculated for the five different sets of images is shown in Figure 8. After obtaining the charge we are able to calculate what the electric field is at the height of the orbiting particle using Eq. (8)

$$Z_d = g2\pi\rho a^3 h_b^2 / 3e(V_p - V_b)(h_b - h_{eq}) \quad (7)$$

$$E = \frac{F_e}{Q} \quad (8)$$

V. DISCUSSION/ANALYSIS

From Experiment One it was found that the slightly larger specimens and specimens that are brighter than the other particles are most likely two to four particles coagulating. Particle coagulates that orbit also spin, which means the particle coagulates rotate about their own axis, and the spin of the particle coagulate is what induces the orbit [15]. It is also assumed that the only dust specimens that orbit are asymmetric agglomerated particles (particle coagulates) [15]. The asymmetry and spin of particle one in experiment one is what is thought to have caused the large amount of movement in the x direction. This means the findings from experiment one are supported by literature on rotation of particles, see source [15]. Knowing this, the observed orbiting structure in experiment two is also a coagulate of particles rather than a single particle. It is thought that particles can exist in a three dimensional region in the phase space of the glass box where $mg=QE$ rather than the plane where $mg=QE$ when no glass box is present. This is a concept currently being explored by the Center for Astrophysics, Space Physics, and Engineering Research at Baylor University. This concept explains why the particle coagulate could be rearranged to a different position in the particle chain by making the chain unstable and then stabilizing the chain again by increasing and lowering power. The orbiting particle coagulate acts as a small probe that maps the sheath region. This is important because a direct measurement of this region has not yet been found. It was shown in section IV how to find the electric field of the sheath at the height of the particle coagulate by using the charge of the coagulate in experiment three and the electric force in experiment four. The electric force was also calculated in experiment two to ensure that the results agreed within error. Rearranging the chain for the coagulate to be at different heights would allow the electric field to be mapped within the region of the box where $mg=QE$.

VI. CONCLUSION

A. Particle Coagulates

There are three main ways in which particles were distinguished from coagulates. First, the laser-scattered light of the specimen is larger than that of particles. Second, the

size of the specimen may help distinguish a particle coagulate from a particle. As stated in section IV, the particle occupied one pixel while the particle coagulate occupied nine pixels. Third, movement of particle coagulates tends to be different than particles within the glass box. A particle coagulate may move much more in the x direction compared to a particle when changing the power and keeping all other parameters constant. Orbiting specimens are also found to be coagulates. This occurs due to the asymmetry of the coagulate.

B. Mapping the Electric Field

Using a dust chain within a glass box that has a particle coagulate orbiting around the axis of the chain allows the electric field of the sheath region to be mapped. Using the frequency and radius of the orbit one may obtain the angular momentum of the coagulate, torque acting on the coagulate, and the electrostatic force acting on the coagulate. The charge of the coagulate can also be estimated using two mathematical equations. This information allows us to find the electric field at the height of the coagulate. Information about the charge of the particle and the sheath region of the glass box were obtained through the experiments done in this paper. This is important because it helps reach the ultimate goal of understanding the conditions within the glass box.

C. Future Work

The free fall experiment was used to calculate the electric force acting on the orbiting particle. The trajectories of the falling particles were measured to find acceleration. The motion of the particle can be found using Eq. (9) from [6] where β was calculated to be 4.7s^{-1} . Using this information, results from the experiments covered in this paper should be compared with a well-known and established method of finding the electric field values within the glass box. Although the published method [6] did not use a glass box, it would still be useful to compare results.

$$m_D \ddot{z} = F_E(z) - m_D g - m_D \beta \dot{z} \quad (9)$$

In experiment one, the particles' movement was monitored as the power was lowered. The power was being manually lowered which created a decrease in power that was not constant. This can be observed in Figures 6 and 7 via luminosity. In order to create a more controlled, precise version of this experiment it would be useful to create a program that has the computer lower the power at a given rate. This program should also be able to communicate with LabVIEW or in LabVIEW so the plasma power and electronic data can be monitored while the power is lowered.

In experiment one the size of the particle coagulate was observed to be greater than the size of the particle. However, exact information about the coagulate size and number of particle in the coagulate could be obtained. Finding these details would allow a more precise measurement of the electric field at the height of the orbiting coagulate, which would give a more precise mapping of the sheath.

It is important that the results from mapping the electric field within the phase space using gold dust be compared to mapping the same space using MF particles, this will provide information about how conduction affects these phase space

conditions. In this paper it was discussed how to find the electric field within the sheath region of the $\frac{1}{2}$ inch box. It would be useful for a model of the electric field at different heights to be created using different particle sizes, different powers, and different glass box sizes. This can be done by anyone with access to a GEC RF Reference Cell.

ACKNOWLEDGMENTS

Kristin J. Sperzel thanks Hannah Sabo, Kevin Liang, and Jesse Kimmery for discussing aspects of the experiments that helped me obtain results from the data. The author thanks Ryan Koehler for helping edit this paper. The author also thanks Brandon Harris for helping with the computational aspects of this project. A big thank you to Mike Cook and Jimmy Schmoke for helping with the lab and lab computers. Finally, the author thanks Baylor University and the CASPER program for this experience and opportunity to learn and do research.

REFERENCES

- [1] W.-D. Kraeft and M. Schlanges, *Quantum Statistics of Nonideal Plasmas*. Springer, 2005.
- [2] D. A. Gurnett and A. Bhattacharjee, *Introduction to Plasma Physics: With Space and Laboratory Applications*. Cambridge University Press, 2005.
- [3] J. Kong, K. Qiao, J. Carmona-Reyes, A. Douglass, Z. Zhang, L. S. Matthews, and T. W. Hyde, "Vertical Interaction Between Dust Particles Confined in a Glass Box in a Complex Plasma," *IEEE Transactions on Plasma Science*, vol. 41, no. 4, pp. 794–798, 2013.
- [4] J. Kong, T. W. Hyde, L. Matthews, K. Qiao, Z. Zhang, and A. Douglass, "One-dimensional vertical dust strings in a glass box," *Phys. Rev. E*, vol. 84, no. 1, p. 016411, Jul. 2011.
- [5] Morfill, G. E., and Thomas, H., 1996, *J. Vac. Sci. Technol. A* 14, 490; Morfill, G. E., Ivlev, A. V., Khrapak, S. A., Klumov, B. A., Rubin-Zuzic, M., Konopka, U., and Thomas, H. M., 2004, *Contrib. Plasma Phys.* 44, 450.
- [6] A. Douglass, V. Land, K. Qiao, L. Matthews, and T. Hyde, "Determination of the levitation limits of dust particles within the sheath in complex plasma experiments," *Physics of Plasmas*, vol. 19, no. 1, pp. 013707–013707–8, Jan. 2012.
- [7] M. Lampe, G. Joyce, and G. Ganguli, "Structure and dynamics of dust in streaming plasma: dust molecules, strings, and Crystals," *IEEE Transactions on Plasma Science*, vol. 33, no. 1, pp. 57–69, 2005.
- [8] R. J. Proccassini, C. K. Birdsall, and E. C. Morse, "A fully kinetic, self-consistent particle simulation model of the collisionless plasma-sheath region," *Physics of Fluids B: Plasma Physics*, vol. 2, no. 12, pp. 3191–3205, Dec. 1990.
- [9] B. W. J. A. A Samarian, "Sheath measurement in rf-discharge plasma with dust grains," *Physics Letters A*, vol. 287, pp. 125–130.
- [10] P. Hartmann, A. Douglass, J. C. Reyes, L. S. Matthews, T. W. Hyde, A. Kovács, and Z. Donkó, "Crystallization Dynamics of a Single Layer Complex Plasma," *Phys. Rev. Lett.*, vol. 105, no. 11, p. 115004, Sep. 2010.
- [11] P. Hartmann, A. Douglass, J. C. Reyes, L. S. Matthews, T. W. Hyde, A. Kovács, and Z. Donkó, "Crystallization Dynamics of a Single Layer Complex Plasma," *Phys. Rev. Lett.*, vol. 105, no. 11, p. 115004, Sep. 2010.
- [12] P. J. Hargis, K. E. Greenberg, P. A. Miller, J. B. Gerardo, J. R. Torczynski, M. E. Riley, G. A. Hebner, J. R. Roberts, J. K. Olthoff, J. R. Whetstone, R. J. Van Brunt, M. A. Sobolewski, H. M. Anderson, M. P. Splichal, J. L. Mock, P. Bletzinger, A. Garscadden, R. A. Gottscho, G. Selwyn, M. Dalvie, J. E. Heidenreich, J. W. Butterbaugh, M. L. Brake, M. L. Passow, J. Pender, A. Lujan, M. E. Elta, D. B. Graves, H. H. Sawin, M. J. Kushner, J. T. Verdeyen, R. Horwath, and T. R. Turner, "The Gaseous Electronics Conference radio-frequency reference cell: A defined parallel-plate radio-frequency system for experimental and theoretical studies of plasma-processing discharges," *Review of Scientific Instruments*, vol. 65, no. 1, p. 140, 1994.
- [13] Y. Ivanov and A. Melzer, "Particle positioning techniques for dusty plasma experiments," *Rev Sci Instrum*, vol. 78, no. 3, p. 033506, Mar. 2007.
- [14] L. S. Matthews, B. Shotorban, and T. W. Hyde, "Cosmic Dust Aggregation with Stochastic Charging," arXiv e-print 1303.5263, Mar. 2013.
- [15] R. P. D. G. V. Paeva, "Rotation of particles trapped in the sheath of a radio-frequency capacitively coupled plasma," *Plasma Science, IEEE Transactions on*, no. 2, pp. 601 – 606, 2004.
- [16] "Ultrahigh Vacuum Chamber-GEC Reference Cell," *IHS GlobalSpec*, 2013. [Online]. Available: http://www.globalspec.com/FeaturedProducts/Detail/NorCalProducts/57898/GEC_Reference_Cell. [Accessed: 05-Aug-2013].

Kristin J. Sperzel was born in Maple Grove, MN, in 1991. She is currently an undergraduate mathematics major and physics minor at St. Cloud University, St. Cloud, MN. She is a member of the Physics Club at St. Cloud State University and also enjoys running. She is a member of the 2013 Center for Astrophysics, Space Physics, and Engineering Research program at Baylor University, Waco, TX.

Jorge Carmona-Reyes received the B.S. degree in physics from Southern Nazarene University, Bethany, OK, and the M.S. degree in physics from Baylor University, Waco, TX. He is currently with Baylor University, where he is an Assistant Research Scientist in the Center for Astrophysics, Space Physics and Engineering Research.

Lorin S. Matthews was born in Paris, TX, in 1972. She received the B.S. and Ph.D. degrees in physics from Baylor University, Waco, TX, in 1994 and 1998, respectively. She is currently an Assistant Professor with the Physics Department, Baylor University. Previously, she worked with Raytheon Aircraft Integration Systems where she was the Lead Vibroacoustics Engineer on NASA's SOFIA (stratospheric observatory for infrared astronomy) project.

Truell W. Hyde (M'00) was born in Lubbock, TX, in 1956. He received the B.S. degree in physics and mathematics from Southern Nazarene University, Bethany, OK, in 1978 and the Ph.D. degree in theoretical physics from Baylor University, Waco, TX, in 1988. He is currently with Baylor University where he is the Director of the Center for Astrophysics, Space Physics & Engineering Research (CASPER), a Professor of physics, and the Vice Provost for Research for the University. His research interests include space physics, shock physics and waves, and nonlinear phenomena in complex (dusty) plasmas.